

IP₃ receptors – lessons from analyses *ex cellula*

Ana M. Rossi and Colin W. Taylor*

Department of Pharmacology, Tennis Court Road, Cambridge, CB2 1PD, UK

* Author for correspondence: cwt1000@cam.ac.uk

Running title

IP₃ receptors

Key words

Bilayer recording; Ca²⁺ channel; Endoplasmic reticulum; Ion channel structure; IP₃ receptor;
Nuclear patch-clamp; Permeabilized cell; Radioligand binding; Ryanodine receptor.

ABSTRACT

Inositol 1,4,5-trisphosphate receptors (IP₃Rs) are widely expressed intracellular channels that release Ca²⁺ from the endoplasmic reticulum (ER). We review how studies of IP₃Rs removed from their intracellular environment (*‘ex cellula’*), alongside similar analyses of ryanodine receptors, have contributed to understanding IP₃R behaviour. Analyses of permeabilized cells demonstrated that the ER is the major intracellular Ca²⁺ store, and that IP₃ stimulates Ca²⁺ release from it. Radioligand binding confirmed that the 4,5-phosphates of IP₃ are essential for activating IP₃Rs, and facilitated IP₃R purification and cloning, which paved the way to structural analyses. Reconstitution of IP₃Rs into lipid bilayers and patch-clamp recording from the nuclear envelope established that IP₃Rs have a large conductance and select weakly between Ca²⁺ and other cations. Structural analyses are now revealing how IP₃ binding to the N-terminus of the tetrameric IP₃R opens the pore ~7nm away from the IP₃-binding core (IBC). Communication between the IBC and pore passes through a nexus of interleaved domains contributed by structures associated with the pore and cytosolic domains, which together contribute to a Ca²⁺-binding site. These structural analyses provide a plausible explanation for the suggestion that IP₃ gates IP₃Rs by first stimulating Ca²⁺ binding, which leads to pore opening and Ca²⁺ release.

Introduction

Inositol 1,4,5-trisphosphate receptors (IP₃Rs) and ryanodine receptors (RyR) are the two major families of intracellular Ca²⁺-release channels in animal cells (**Fig. 1A**). IP₃Rs are expressed in most cells, whereas RyRs have a more restricted distribution. RyRs are most abundant in excitable cells, notably in striated muscle, where they contribute to excitation-contraction coupling (**Fig. 1A**) (Van Petegem, 2014). In this review, we focus on IP₃Rs, and how methods applied to IP₃Rs removed from intact cells have contributed to our understanding of IP₃R behaviour. Progress with understanding IP₃Rs and RyRs has developed in parallel, and with this progress it became clear that the two families share structural and functional features (Baker et al., 2017; Seo et al., 2012). Hence, despite our focus on IP₃Rs, we draw also on evidence from analyses of RyRs.

Classic work by Sydney Ringer demonstrated that cardiac muscle contraction requires extracellular Ca²⁺ (Ringer, 1883). This was, with benefit of hindsight, the first of many studies to show that the contributions to physiological responses of extracellular Ca²⁺ and Ca²⁺ held within intracellular stores are entangled. For cardiac muscle, depolarization of the plasma membrane (PM) causes voltage-gated Ca²⁺ channels (Ca_v1.2) to open, and the local increase in cytosolic free Ca²⁺ concentration [Ca²⁺]_c is then amplified by Ca²⁺-induced Ca²⁺ release (CICR) through type 2 ryanodine receptors (RyR2) in the sarcoplasmic reticulum (Bers, 2002) (**Fig. 1A**). CICR and the local Ca²⁺ signalling that is required to avoid CICR from becoming explosive have become recurrent themes in Ca²⁺ signalling (Rios, 2018). Fluorescent Ca²⁺ indicators and optical microscopy now allow Ca²⁺ sparks, local Ca²⁺ signals evoked by a small cluster of RyRs, to be measured with exquisite subcellular resolution in cardiac muscles (Cheng and Lederer, 2008). However, it was studies of permeabilized cells ('skinned' fibres) that provided the first evidence for CICR in muscle (Endo et al., 1970; Fabiato and Fabiato, 1979). Analyses of RyRs that were reconstituted into planar lipid bilayers first showed that RyRs form large-conductance cation channels that are biphasically regulated by cytosolic Ca²⁺ (Lai et al., 1988; Meissner, 2017). Finally, analyses of RyR fragments by X-ray crystallography (Van Petegem, 2014) and of complete RyRs by cryo-electron microscopy (des Georges et al., 2016; Efremov et al., 2015; Peng et al., 2016; Yan et al., 2015; Zalk et al., 2015) are revealing the structural basis of RyR behaviour.

Progress towards understanding the second major family of intracellular Ca²⁺-release channels, the IP₃Rs, began with an influential review in which a causal link between receptor-stimulated turnover of phosphatidylinositol and Ca²⁺ signalling was proposed (Michell, 1975). Subsequent work established that many receptors stimulate phospholipases C, which

cleave phosphatidylinositol 4,5-bisphosphate to produce IP₃ and diacylglycerol (Berridge, 1993) (**Fig. 1A**). IP₃ provides the link to Ca²⁺ signalling; not, as first envisaged by directly stimulating Ca²⁺ entry across the PM (Michell, 1975), but by stimulating Ca²⁺ release from the endoplasmic reticulum (ER) through IP₃Rs (Berridge and Irvine, 1984; Streb et al., 1983). Another influential review suggested the link between IP₃-evoked Ca²⁺ release and Ca²⁺ entry across the PM. This review proposed that loss of Ca²⁺ from the ER stimulated Ca²⁺ entry (Putney, 1986). The workings of this store-operated Ca²⁺ entry (SOCE) pathway are now clear: dissociation of Ca²⁺ from the luminal EF-hand motif of a protein embedded in the ER membrane, stromal interaction molecule 1 (STIM1), causes STIM1 to oligomerize and expose a cytosolic domain, through which it stimulates opening of a Ca²⁺-selective channel in the PM (Feske et al., 2006; Prakriya and Lewis, 2015). The Ca²⁺ channel that mediates SOCE is a hexameric assembly of Orai subunits (Hou et al., 2012; Yen and Lewis, 2018), grandiloquently named from Greek mythology after the keepers of Heaven (Feske et al., 2006).

IP₃Rs and RyRs are biphasically regulated by cytosolic Ca²⁺ (Bezprozvanny et al., 1991). For IP₃Rs exposed to IP₃, a modest increase in [Ca²⁺]_c stimulates opening, whereas higher [Ca²⁺]_c are inhibitory (Foskett et al., 2007; Iino, 1990). Hence IP₃Rs, at least once they have bound IP₃ (Alzayady et al., 2016), can, like RyRs, mediate CICR (**Fig. 1B,C**). As with RyRs, IP₃Rs assemble into clusters, within which opening of one IP₃R ignites the activity of its neighbours to generate local 'Ca²⁺ puffs' (**Fig. 1C**) (Smith and Parker, 2009; Thillaiappan et al., 2017), analogous to Ca²⁺ sparks in muscle. These behaviours illustrate some of the many similarities between IP₃Rs and RyRs, which include their close structural relationship (Baker et al., 2017; Seo et al., 2012; Van Petegem, 2014). Although IP₃Rs and RyRs are the major intracellular Ca²⁺-release channels, they are not the only intracellular Ca²⁺ channels (**Box 1**).

The productive interplay between studies of minimally perturbed tissue, facilitated by a plethora of Ca²⁺ indicators (Lock et al., 2015), fluorescent proteins (Rodriguez et al., 2017) and fluorescence microscopy techniques (Thorn, 2016), alongside analyses of cellular components has shaped our understanding of Ca²⁺ signalling. Here, we consider how analyses of IP₃Rs conducted outside their normal intracellular environment (*ex cellula*) have advanced our understanding of IP₃-evoked Ca²⁺ signals. We begin by considering how analyses of permeabilized cells established that the ER is the major intracellular Ca²⁺ store and that IP₃ releases Ca²⁺ from it. Radioligand binding analyses then both identified the sites to which IP₃ binds to activate IP₃Rs and paved the way to structural studies, which we show are now coming close to revealing how IP₃ binding causes the pore of the IP₃R to open. We

conclude by considering the contributions of electrophysiological recordings to our understanding of IP₃R gating.

Lessons from permeabilized cells

Permeabilized cells allow the Ca²⁺ content of intracellular organelles to be measured under conditions where the intracellular environment can be precisely controlled. To achieve this control, the PM must be disrupted without unduly perturbing organelles (Schulz, 1990). The permeabilized cells are then bathed in medium that mimics cytosol, notably in its low [Ca²⁺]_c (~100 nM). Electroporation (Knight, 1981; Xie et al., 2013) and a variety of chemical means have been used to selectively permeabilize the PM. The chemicals achieve their PM-selectivity by interacting with cholesterol (e.g. saponin, digitonin, β-escin), which is enriched in the PM (Wassler et al., 1987), or as pore-forming toxins (e.g. α-toxin, streptolysin-O) that are too large to pass through their own pores (Schulz, 1990).

After a protracted controversy (Babcock et al., 1979; Dehay et al., 1980), analyses of permeabilized cells established that the ER, rather than mitochondria, is the major intracellular Ca²⁺ store in animal cells (Burgess et al., 1983). In an elegant study, saponin-permeabilized hepatocytes were bathed in cytosol-like medium with Ca²⁺ buffered to mimic the [Ca²⁺]_c of an unstimulated cell. Each permeabilized cell was then shown to have the same Ca²⁺ content as an intact cell, and critically all of that Ca²⁺ was in the ER (Burgess et al., 1983). Hence, it is the ER from which most extracellular stimuli evoke Ca²⁺ release.

Analyses of insect salivary glands demonstrated that phosphoinositide turnover was required for extracellular stimuli to evoke Ca²⁺ signals (Berridge and Fain, 1979), and showed that IP₃ was the first cytosolic product of receptor-stimulated phosphoinositide hydrolysis (Berridge, 1983). Hence, IP₃ emerged as the likely messenger that links receptors in the PM to Ca²⁺ release from the ER (**Fig. 1A**). Permeabilized cells again provided the decisive experiment: addition of IP₃ to permeabilized pancreatic acinar cells stimulated release of Ca²⁺ from a non-mitochondrial Ca²⁺ store (Streb et al., 1983). It is now universally accepted that most IP₃Rs reside in ER membranes, but IP₃Rs can also mediate Ca²⁺ release from the Golgi apparatus (Aulestia et al., 2015; Pinton et al., 1998), the nuclear envelope (Foskett et al., 2007; Rahman et al., 2009; Stehno-Bittel et al., 1995) and perhaps from a nucleoplasmic reticulum (Echevarria et al., 2003). In some cells, a few IP₃Rs (typically only 2-3 IP₃Rs per cell) are also expressed in the PM, where they mediate Ca²⁺ entry (Dellis et al., 2006; Dellis et al., 2008). In many studies, though not in all (Watras et al., 1991), the ER Ca²⁺ release evoked by IP₃ was shown to be positively cooperative (eg, Champeil et al., 1989; Marchant and Taylor,

1997; Meyer et al., 1988), suggesting a need for IP₃ to bind to several IP₃R subunits before the channel can open. A recent study using concatenated IP₃R subunits showed that a defective IP₃-binding site in only one of the four subunits prevents IP₃R activation (Alzayady et al., 2016), leading to the conclusion that all four subunits of an IP₃R must bind IP₃ before the channel can open.

But IP₃ binding is not alone sufficient to stimulate Ca²⁺ release through IP₃Rs. Instead, IP₃ binding primes IP₃Rs to bind Ca²⁺, and Ca²⁺ binding then causes the channel to open (Adkins and Taylor, 1999; Marchant and Taylor, 1997) (**Fig. 1B**). Hence, IP₃Rs require binding of two ligands, IP₃ and Ca²⁺, to open. This dual regulation endows IP₃Rs with their capacity to mediate regenerative Ca²⁺ signals through CICR. Again, it was analyses of permeabilized cells that provided the first evidence that Ca²⁺ release through IP₃Rs is regulated by [Ca²⁺]_c (Iino, 1987). High-resolution optical analyses of Ca²⁺ signals later revealed that within intact cells, IP₃-evoked Ca²⁺ signals originate from elementary units that comprise a small cluster of IP₃Rs (Smith and Parker, 2009; Thillaiappan et al., 2017). Opening of the first IP₃R within a cluster is proposed to rapidly ignite the activity of some of its neighbours by CICR to generate a Ca²⁺ puff (**Fig. 1C**). As the stimulus intensity increases, Ca²⁺ spreading from one Ca²⁺ puff to another IP₃R cluster can initiate further Ca²⁺ puffs, allowing the signal to spread across the cell as a regenerative Ca²⁺ wave (Marchant et al., 1999). The frequency of these global signals then increases with stimulus intensity (Thurley et al., 2014).

Structure-activity relationships (SAR), established by comparing the activities of a range of structurally-related chemical stimuli, are often used to probe the recognition properties of receptors. SAR analyses of the effects of IP₃ analogues on Ca²⁺ release from permeabilized cells provided the first evidence that dephosphorylation of IP₃ to (1,4)IP₂ terminates IP₃ activity (Burgess et al., 1984). The (1,3,4,5)IP₄ that is produced when IP₃ is phosphorylated by IP₃ 3-kinase was proposed to regulate IP₃Rs (Loomis-Husselbee et al., 1996), but it is now clear that this phosphorylation also inactivates IP₃ signalling through IP₃Rs (Bird and Putney, 1996; Saleem et al., 2012). Hence, both endogenous pathways for IP₃ metabolism effectively inactivate IP₃ signalling to IP₃Rs (**Fig. 1A**). SAR analyses of many analogues of IP₃ and adenophostin A, a fungal metabolite that binds with high-affinity to IP₃Rs (Takahashi et al., 1994), established that a key feature of IP₃R agonists is the presence of a vicinal 4,5-bisphosphate moiety (**Fig. 1D**) (Rossi et al., 2010; Rossi et al., 2009; Saleem et al., 2012). All active inositol phosphate analogues have this 4,5-vicinal bisphosphate moiety (**Fig. 1D**).

There are no wholly selective antagonists of IP₃Rs. Some ligands (heparin, 2-aminoethoxydiphenylborane (2-APB), Xestospongins C and caffeine) have utility, but they all

lack selectivity. Furthermore, heparin is not membrane-permeant, and results with Xestospongin C are inconsistent (see Saleem et al., 2014). Addition of large substituents to the 2-*O*-position of IP₃ produces partial agonists. Partial agonists are ligands that, once they have bound to IP₃R, are less effective in causing the channel to open than full agonists like IP₃ (Rossi et al., 2009). These SAR analyses of 2-modified analogues of IP₃, again relying heavily on permeabilized cells, have both confirmed the importance of the extreme N-terminal region of the IP₃R (the suppressor domain, SD, **Fig. 1E**) in IP₃R activation and they suggest systematic strategies towards developing high-affinity antagonists of IP₃Rs. There is, therefore, a long history of experiments using permeabilized cells illuminating our understanding of IP₃-evoked Ca²⁺ release. These studies first identified ER as the major intracellular Ca²⁺ store, they showed that IP₃ evokes Ca²⁺ release from the ER, and that IP₃Rs are regulated by Ca²⁺. Furthermore, they defined the biochemical steps that inactivate IP₃ and, through SAR analyses, they have provided ligands that have contributed to understanding the mechanisms of IP₃R activation.

Analyses of IP₃ binding to IP₃Rs

Binding of IP₃ to the four binding sites of the IP₃R initiates the conformational changes that culminate in opening of the Ca²⁺-permeable pore (Alzayady et al., 2016; Chandrasekhar et al., 2016). These IP₃ binding events are usually analysed by means of radioligand binding, which allows determination of binding affinities (as equilibrium dissociation constants, K_D) for ³H-IP₃ or any competing ligand, but there are a variety of other methods (**Fig. 2, Box 2**). K_D values are important for comparison with functional analyses in revealing how ligands activate IP₃Rs. Such analyses were, for example, critical in showing that the vicinal 4,5-bisphosphate of IP₃ is essential for activity, whereas the 1-phosphate improves binding affinity (**Fig. 1D**) (Nahorski and Potter, 1989). Comparisons of SAR with binding analyses can also establish which bound ligands most effectively open the channel. Our comparisons of functional and ³H-IP₃ equilibrium-competition binding analyses, for example, established that whereas IP₃ is a full agonist that effectively gates the IP₃R, other modified analogues of IP₃ bind with high-affinity to IP₃R, but they are much less effective in causing the channel to open (Rossi et al., 2009). These partial agonists provide insight into the mechanisms of IP₃R activation by demonstrating how large moieties at the 2-position of IP₃ attenuate IP₃R activation, and they suggest strategies for development of analogues that bind without activating IP₃Rs (i.e. antagonists).

Binding analyses also allow IP₃R properties to be addressed under conditions where IP₃-evoked Ca²⁺ release is not retained. This opportunity is particularly important during purification of IP₃R for structural studies using either IP₃R fragments for X-ray crystallography (Bosanac et al., 2002; Bosanac et al., 2005; Hamada et al., 2017; Lin et al., 2011; Seo et al., 2012) or, after detergent-solubilization of complete IP₃R, for single-particle analysis by cryo-EM (Fan et al., 2015; Paknejad and Hite, 2018). In subsequent sections, we review progress towards understanding how IP₃ binding leads to opening of the IP₃R pore.

IP₃ initiates IP₃R activation by binding to the IP₃-binding core

The route to IP₃R structures began with the identification of specific, high-affinity, intracellular ³²P-IP₃-binding sites with recognition properties that matched those expected of the receptor through which IP₃ evoked Ca²⁺ release (Baukal et al., 1985; Spät et al., 1986). Subsequent studies established that heparin competed with ³H-IP₃ for these binding sites (heparin is a competitive antagonist of IP₃), and that the sites were abundant in Purkinje cells of cerebellum (Worley et al., 1987). Together, these observations allowed IP₃R to be purified from cerebellum using heparin-chromatography (Maeda et al., 1988; Supattapone et al., 1988). Functional reconstitution of the purified protein then established that it was alone sufficient to form an IP₃-gated Ca²⁺ channel (Ferris et al., 1989; Maeda et al., 1991). Many additional proteins were later shown to associate with IP₃R and modulate their responses to IP₃ (Prole and Taylor, 2016). Screening of cDNA libraries from cerebellum then provided the complete primary sequence of IP₃R1 (Furuichi et al., 1989; Mignery et al., 1989), and soon afterwards the other two IP₃R subtypes, IP₃R2 (Südhof et al., 1991) and IP₃R3 (Blondel et al., 1993) were identified. Subsequent studies established that the three IP₃R subunits (IP₃R1-3) assemble to form homo-tetrameric and hetero-tetrameric channels (Monkawa et al., 1995), and they confirmed that the core properties of all IP₃R subtypes are similar: each forms a large-conductance Ca²⁺-permeable channel that is gated by binding of IP₃ and Ca²⁺ (Foskett, 2010), and each generates Ca²⁺ puffs (Mataragka and Taylor, 2018). The subtypes are, however, differentially expressed, and they differ in their affinities for IP₃ (Iwai et al., 2007), sensitivity to Ca²⁺ regulation (Foskett, 2010) and in whether they are modulated by additional regulators (Prole and Taylor, 2016). Furthermore, the functional consequences of mutant or defective IP₃R differ among subtypes (see Terry et al., 2018). IP₃R1 has so far been the major focus of the structural studies.

Deletion analyses (Mignery and Südhof, 1990) and expression of IP₃R fragments in bacteria (Yoshikawa et al., 1996) established that each IP₃R subunit has a single IP₃-binding site

formed by residues, the IBC (residues 224-604), towards the N-terminal of the primary
 sequence (~2750 residues) (**Fig. 1E**). The identification of four IP₃-binding sites in each
 IP₃R, and the demonstration that all four are required for IP₃ to evoke Ca²⁺ release (Alzayady
 et al., 2016), provided an explanation for the widely observed cooperative responses to IP₃
 (Champeil et al., 1989; Meyer et al., 1988; Parker and Miledi, 1989). Subsequent studies
 identified residues within the IBC that are required for IP₃ binding, notably the residues that
 bind to the critical 4- and 5-phosphate groups of IP₃ (Furutama et al., 1996). These residues
 are conserved in IP₃Rs, but not in RyRs (Bosanac et al., 2002; Seo et al., 2012). It was also
 shown that the SD inhibits IP₃ binding (Uchida et al., 2003), which aligns with the
 importance of the SD in coupling IP₃ binding to channel gating (Rossi et al., 2009): IP₃Rs
 without an SD bind IP₃ with high affinity, but they do not release Ca²⁺ (Uchida et al., 2003).
 High-resolution crystal structures of N-terminal fragments of the IP₃R directly revealed both
 the determinants of IP₃ binding and the initial steps in IP₃R activation. The two domains (α
 and β) of the IBC form a clam-like structure, within which conserved residues bind to IP₃
 (Bosanac et al., 2002). The 1- and 5-phosphates of IP₃ interact predominantly with residues in
 IBC- α , whereas the 4-phosphate interacts with IBC- β (**Fig. 1D,E**). Interaction of the critical
 4- and 5-phosphates with opposing sides of the clam allows IP₃ to partially close the clam and
 initiate IP₃R activation (Hamada et al., 2017; Lin et al., 2011; Paknejad and Hite, 2018; Seo
 et al., 2012). That interpretation, which elegantly reveals the structural basis of the SAR, is
 supported by results with an adenophostin A analogue in which an alternative contact with
 the α -domain substitutes for loss of the usual phosphate (Sureshan et al., 2012).
 In the isolated N-terminal domain, the SD is firmly anchored to IBC- α by an extensive
 interface and more loosely associated with IBC- β (**Fig. 1E**). Hence, when IP₃ causes the IBC
 clam to close, the SD moves with IBC- α and that was predicted to disrupt interaction of an
 exposed SD loop, the 'hot spot' loop (Yamazaki et al., 2010) with IBC- β of a neighbouring
 subunit (Seo et al., 2012). In RyR too, these inter-subunit interactions between N-terminal
 domains are weakened during receptor activation (des Georges et al., 2016). The resulting
 weakening of interactions between subunits may contribute to channel gating. This is
 supported by evidence that Ca²⁺-binding protein 1 (CaBP1), which inhibits IP₃R gating,
 rigidifies these interactions between IP₃R subunits (Li et al., 2013). However, within the
 constraints of a full-length IP₃R, strong inter-subunit interactions between the SD and IBC- β
 might constrain the SD, such that IBC- α moves when IP₃ closes the clam (Paknejad and Hite,
 2018). Identification of the sites to which IP₃ binds, which relied heavily on radioligand

binding analyses, set the scene for the structural analyses that seek to understand how IP₃ binding opens the pore of the IP₃R. We consider recent progress with such structural analyses in the next section.

Structures of complete IP₃ and ryanodine receptors

Structures determined by single-particle analysis of cryo-EM images of the complete IP₃R1 in a closed state (Fan et al., 2015), of IP₃R3 with and without IP₃ and Ca²⁺ bound (Paknejad and Hite, 2018), and of RyRs in different states (des Georges et al., 2016; Efremov et al., 2015; Peng et al., 2016; Yan et al., 2015; Zalk et al., 2015) have begun to reveal the workings of the pore regions of these related channels. The results also tentatively suggest how IP₃ binding might lead to opening of the IP₃R pore.

The IP₃R has a structure reminiscent of a square mushroom. Much of the stalk is embedded in the ER membrane and the cap, with a diameter of ~25 nm, extends at least 13 nm into the cytosol (Fan et al., 2015). The large size is significant because it might exclude IP₃Rs from the narrow junctions between ER and the PM (Thillaiappan et al., 2017), whereas at other junctions, between ER and mitochondria for example (Csordas et al., 2018), it places the head of the IP₃R, from which Ca²⁺ exits, very close to the neighbouring organelle.

The cytosolic entrance to the central cavity of the IP₃R is surrounded by the N-terminal domains (SD and IBC-β, **Fig. 3**). IBC-α forms part of a larger domain (ARM1) that curves to the edge of the cap and interacts with two large curved domains (ARM2 and ARM3) that comprise most of the remaining cytosolic structure and form the underside of the mushroom (**Fig. 3**). Within the ER membrane, there are 24 trans-membrane domains (TMDs), six from each subunit (Fan et al., 2015). However, recent structural analyses of both IP₃R (Paknejad and Hite, 2018) and RyR1 (des Georges et al., 2016) identified a pair of additional helices (between TMD1 and 2 of IP₃R3) that challenge the accepted view that there are six TMDs per subunit. The TMD region, similar in structure to voltage-gated ion channels, is very similar (though not identical) (Baker et al., 2017) in RyRs and IP₃Rs. The ion-conducting path is lined by the four tilted TMD6 helices and a short (~1 nm) ‘selectivity filter’ at the luminal end through which hydrated cations must pass in single-file. The selectivity filter, its supporting pore-loop helix and a flexible luminal loop are all formed by residues linking TMD5 to TMD6. Near the cytosolic end of TMD6, a narrow hydrophobic constriction blocks the movement of ions in the closed channel (Fan et al., 2015) (**Fig. 3**). The hydrophobic side chains of these residues must move for the pore to open. Opening of the RyR is associated with splaying and bowing of TMD6, such that the hydrophobic side-chain of a residue that

occludes the cytosolic end of the closed pore is displaced, opening a hydrophilic path that allows passage of a hydrated Ca^{2+} ion. Similar mechanisms may be associated with opening of the IP_3R pore.

TMD6 is supported by TMD5, which is buttressed by the TMD1-4 bundle of the adjacent subunit. The short cytosolic TMD4-5 helical linker aligns along the ER membrane behind the TMD6 helices holding them in place. In the closed RyR1 channel, this linker tightly encircles the cytosolic end of the TMD6 bundle restricting its movement, but this grip is relaxed as the channel opens freeing TMD6 to move, and allowing the pore to dilate (des Georges et al., 2016). In both IP_3R and RyR, TMD6 extends well beyond the ER membrane (~1.5 nm in IP_3R) and then terminates in a pair of short α -helices (the linker domain, LNK, in IP_3R) that includes a Zn^{2+} -finger motif that aligns parallel with the ER membrane (des Georges et al., 2016; Fan et al., 2015; Paknejad and Hite, 2018). In IP_3R , but notably not in RyR, the entwined TMD6 helices then continue beyond the LNK domain to the cap of the mushroom, where each contacts the IBC- β domain of a neighbouring subunit (Fan et al., 2015). Hence, structures formed by the TMD5-6 loop guard the luminal entrance to the pore, whereas the cytosolic vestibule is formed by the extended TMD6. Each of these regions is enriched in acidic residues that probably contribute to the cation selectivity of IP_3R and RyR (des Georges et al., 2016; Fan et al., 2015; Paknejad and Hite, 2018).

A conserved Ca^{2+} -binding site is present in both RyR (des Georges et al., 2016) and IP_3R (Paknejad and Hite, 2018). The site is formed, in the case of IP_3R , by residues near the C-terminal end of ARM3 and by another residue contributed by the LNK domain (**Fig. 3**). In RyR, the equivalent residues are proposed to coordinate the Ca^{2+} required for stimulation (des Georges et al., 2016). The same may hold true for IP_3Rs , but this has yet to be tested. A conserved glutamate residue on the bottom surface of the ARM3 domain (Glu²¹⁰¹ in $\text{IP}_3\text{R1}$) previously suggested to mediate Ca^{2+} regulation of IP_3R (Miyakawa et al., 2001) and RyR (Fessenden et al., 2001), does not contribute to Ca^{2+} binding to this site, but it does stabilize the interaction between the cooperating domains in RyR1 (des Georges et al., 2016). A second Ca^{2+} -binding site was identified in the structure of $\text{IP}_3\text{R3}$, and again it is formed by residues that are contributed by different domains (ARM3 and the α -helical domain linking ARM1 to ARM2) (Paknejad and Hite, 2018) (**Fig. 3**). Formation of both Ca^{2+} -binding sites requires movement of the contributing domains from their positions in the apo-state, so as to bring the Ca^{2+} -coordinating residues into register (Paknejad and Hite, 2018). This important observation is consistent with evidence that IP_3 controls IP_3R gating by regulating Ca^{2+} binding (**Fig. 1B**).

Taken together, structures of full-length IP₃R_s have defined where IP₃ binds, identified Ca²⁺-binding sites that may mediate Ca²⁺ regulation, and established that hydrophobic residues projecting into the pore must move to allow Ca²⁺ to pass.

Towards understanding how IP₃ and Ca²⁺ binding open the IP₃R pore

The only contacts between the large cytosolic structures of the IP₃R and its channel region are the C-terminal end of ARM3 and the LNK domain (**Fig. 3**) (Fan et al., 2015). There are similar contacts in RyR (des Georges et al., 2016). In both IP₃R and RyR, this critical nexus comprises a platform of interleaved structures: the C-terminus of the ARM3 domain (the intervening lateral domain, ILD) forms a ‘thumb-and-fingers’ arrangement of an upper thumb abutting the bulk of ARM3, and an α -helical pair of fingers lying below and forming a cavity into which the LNK domain inserts (**Fig. 3**) (Fan et al., 2015). Mutations within the thumb disrupt IP₃R function (Hamada et al., 2017). The LNK domain also wraps around the thumb and contributes a residue to the Ca²⁺-binding site at the base of the ARM3 domain.

How, then, does IP₃ binding to the IBC cause hydrophobic pore residues some 7 nm distant to move and allow Ca²⁺ to pass from the ER lumen to the cytosol (Fan et al., 2015)? Recalling that IP₃ primes IP₃R_s to bind Ca²⁺, which then triggers channel opening (Adkins and Taylor, 1999) (**Fig. 1B**), it seems reasonable to speculate that IP₃ binding to the IBC is communicated to the Ca²⁺-binding site at the ILD-LNK nexus and thence to the pore (Paknejad and Hite, 2018). IP₃ binding closes the clam-like IBC, and, with IBC- β held firmly in place by inter-subunit interactions at the top of the mushroom, IBC- α moves and initiates conformational changes throughout the associated ARM domains. These changes include disruption of inter-subunit interaction between ARM1 and ARM2 domains, and rotation of the LNK domains (Paknejad and Hite, 2018). Here, the need for the SD is attributed to its role in stabilizing inter-subunit interactions to provide a fixed structure against which movement of IBC- α can leverage conformational changes through the ARM domains (Paknejad and Hite, 2018).

Given the essential role of the SD in IP₃R activation, an alternative possibility was that the direct contact between the SD and ARM3 might mediate communication between N-terminal regions and the ILD. However, the SD-ARM3 interaction occurs through the handle of the hammer-like SD, which can be deleted without impairing IP₃R function (Yamazaki et al., 2010). Another possibility was that interaction between IBC- β and the CTD (which is unique to IP₃R) might communicate IP₃ binding to the LNK domain. However, this scheme is difficult to reconcile with functional IP₃R/RyR chimeras (Seo et al., 2012) since the RyR structure does not have an extended CTD, and with evidence that deletion of residues within

the CTD that interact with IBC- β do not prevent IP₃-evoked Ca²⁺ release (Hamada et al., 2017; Schug and Joseph, 2006). Whatever the exact path from IBC to the ILD-LNK nexus is, IP₃-evoked conformational changes appear to reconfigure the Ca²⁺-binding site formed at the LNK-ARM3 interface to allow Ca²⁺ binding (Paknejad and Hite, 2018), thereby providing a plausible mechanism for IP₃ priming IP₃Rs to respond to Ca²⁺ (**Fig. 1B**). We conclude that analyses of IP₃ binding contributed to defining the SAR for IP₃Rs and to quantitative comparisons of the relationship between binding and channel activation, but most significantly they allowed IP₃Rs to be identified during their purification, which paved the way to cloning and molecular manipulation of IP₃Rs, and to structural studies. The latter have established that IP₃Rs are huge tetrameric structures, wherein IP₃ binding closes a clam-like IBC. That conformational change is communicated to a critical nexus between interleaved structures from the cytosolic and channel domains. IP₃ binding probably stabilizes Ca²⁺ binding to this nexus, leading to re-arrangement of the pore, such that occluding hydrophobic residues are displaced to allow the passage of Ca²⁺ from the ER lumen to the cytosol.

Lessons from planar lipid bilayers and patch-clamp recording

Electrical recordings from ion channels, most often by means of patch-clamp recording (**Box 3**) (Lape et al., 2008; Neher, 1992), allow the openings and closing of single channels to be recorded with sub-millisecond resolution, and they allow their ion permeation properties to be defined. Since the intracellular location of RyR and IP₃R in the ER presents a formidable barrier to such recordings (Jonas et al., 1997), two alternative approaches have been used.

Planar lipid bilayers

The first approach, which involves reconstitution of ER vesicles or solubilized IP₃Rs into planar lipid bilayers, provided the first measurements of currents through IP₃R (Bezprozvanny et al., 1994; Bezprozvanny and Ehrlich, 1994; Bezprozvanny et al., 1991; Ehrlich and Watras, 1988; Maeda et al., 1991). These analyses established that IP₃R, like RyR, are large-conductance cation channels with relatively low-selectivity for Ca²⁺. Both features are important in allowing IP₃R to generate large local cytosolic Ca²⁺ signals: the large conductance allows an open IP₃R to pass ~500,00 Ca²⁺ per second (Foskett et al., 2007), whereas the weak selectivity might allow a counter-flux of K⁺ to dissipate the electrical gradient that is formed as Ca²⁺ leaves the ER and which would otherwise rapidly terminate Ca²⁺ release (Zsolnay et al., 2018). The short, wide selectivity filter and large vestibules with

abundant acidic residues probably provide the structural basis of these ion permeation properties (Fan et al., 2015). Bilayer analyses also confirmed the biphasic regulation of IP₃R1 by cytosolic Ca²⁺ (Bezprozvanny et al., 1991). A potential problem with recordings from planar lipid bilayers is that solubilization and/or reconstitution could lead to loss of accessory proteins or perturbation of structure. Maximal open probabilities recorded from IP₃Rs in bilayers, for example, are much lower than in patch-clamp recordings, and bilayer recordings of IP₃R2 and IP₃R3 failed to capture the inhibitory effect of cytosolic Ca²⁺ (Hagar et al., 1998; Ramos-Franco et al., 2000).

Patch-clamp recording

The second approach to obtaining electrical recordings from IP₃R exploits the fact that the ER is continuous with the outer nuclear membrane (ONM) (**Box 3**) (Dingwall and Laskey, 1992). Hence, patch-clamp recording from the ONM allows analysis of IP₃R in a native membrane, albeit not the ER (Mak et al., 2013; Rahman and Taylor, 2010) (**Box 3**). These recordings, which have been applied to both native and heterologously expressed IP₃Rs (Betzenhauser et al., 2008; Cheung et al., 2010; Foskett et al., 2007; Marchenko et al., 2005; Rahman et al., 2009), confirmed their ion permeation properties and the biphasic regulation of all IP₃R subtypes by Ca²⁺. They have also suggested complex gating schemes wherein IP₃ drives bursts of IP₃R activity by extending the duration of sequences of openings and shortening the gaps between the bursts (Gin et al., 2009; Ionescu et al., 2007).

Another application of nuclear patch-clamp recording is provided by our work, where we showed that IP₃Rs within patches that fortuitously contained several IP₃Rs behave differently to patches with only a single IP₃R (Rahman et al., 2009). This led to our proposal that low concentrations of IP₃, perhaps arising from occupancy of only some of the four IP₃-binding sites, trigger IP₃R clustering (Rahman et al., 2009). The clustered IP₃Rs, we suggest, are better placed than lone IP₃Rs to benefit from CICR when a near neighbour opens to release Ca²⁺ and so provide the second stimulus that is needed for IP₃R opening (**Fig. 1B**). Effects of clustering on the IP₃ and Ca²⁺ sensitivity of IP₃Rs reinforce the propensity of clustered IP₃Rs to amplify Ca²⁺ signals by CICR. These proposals have been challenged (Rahman et al., 2011; Smith et al., 2009; Vais et al., 2011) and our own recent work suggests that even in unstimulated cells there are pre-existing clusters of IP₃Rs, each typically comprising about eight IP₃Rs (Thillaiappan et al., 2017). Our revised proposal therefore envisages that IP₃Rs are, as we have shown, loosely clustered in unstimulated cells (Thillaiappan et al., 2017) and

that IP₃ might then cause IP₃Rs within the cluster to huddle more closely and so be more likely to respond to Ca²⁺ released by a neighbour.

Concluding remarks

Throughout the long history of analyses of intracellular Ca²⁺ signalling, there has been a productive interplay between studies of intact tissues and of biological systems extracted from intact cells (*ex cellula*). These approaches succeeded in showing that the ER is the major intracellular Ca²⁺ store and they identified the enormous channels (RyR and IP₃R) that mediate Ca²⁺ release from the ER. We are now fast approaching an understanding of how IP₃ binding leads, through its interactions with Ca²⁺ binding, to opening of the IP₃R. In parallel with these approaches, developments in optical microscopy have provided opportunities to examine IP₃-evoked Ca²⁺ release with exquisite temporal and spatial resolution in intact cells. We can surely look forward to these analyses converging with structural analyses *in situ* to provide a comprehensive understanding of IP₃Rs in living cells.

Funding

This work was supported by the Wellcome Trust (grant number 101844) and the Biotechnology and Biological Sciences Research Council (grant number BB/P005330/1).

References

- Adkins, C. E. and Taylor, C. W. (1999). Lateral inhibition of inositol 1,4,5-trisphosphate receptors by cytosolic Ca²⁺. *Curr. Biol.* **9**, 1115-1118.
- Alzayady, K. J., Wang, L., Chandrasekhar, R., Wagner, L. E., 2nd, Van Petegem, F. and Yule, D. I. (2016). Defining the stoichiometry of inositol 1,4,5-trisphosphate binding required to initiate Ca²⁺ release. *Sci. Signal.* **9**, ra35.
- Aulestia, F. J., Alonso, M. T. and Garcia-Sancho, J. (2015). Differential calcium handling by the cis and trans regions of the Golgi apparatus. *Biochem. J.* **466**, 455-465.
- Babcock, D. F., Chen, J. L., Yip, B. P. and Lardy, H. A. (1979). Evidence for mitochondrial localization of the hormone-responsive pool of Ca²⁺ in isolated hepatocytes. *J. Biol. Chem.* **254**, 8117-8120.
- Baker, M. R., Fan, G. and Serysheva, II. (2017). Structure of IP₃R channel: high-resolution insights from cryo-EM. *Curr. Opin. Struct. Biol.* **46**, 38-47.

471 **Baukal, A. J., Guillemette, G., Rubin, R., Spat, A. and Catt, K. J.** (1985). Binding sites
 472 for inositol trisphosphate in the bovine adrenal cortex. *Biochem. Biophys. Res.*
 473 *Commun.* **133**, 532-538.

474 **Berridge, M. J.** (1983). Rapid accumulation of inositol trisphosphate reveals that agonists
 475 hydrolyse polyphosphoinositides instead of phosphatidylinositol. *Biochem. J.* **212**, 849-
 476 858.

477 **Berridge, M. J.** (1993). Inositol trisphosphate and calcium signalling. *Nature* **361**, 315-325.

478 **Berridge, M. J. and Fain, J. N.** (1979). Inhibition of phosphatidylinositol synthesis and the
 479 inactivation of calcium entry after prolonged exposure of the blowfly salivary gland to
 480 5-hydroxytryptamine. *Biochem. J.* **178**, 59-69.

481 **Berridge, M. J. and Irvine, R. F.** (1984). Inositol trisphosphate, a novel second messenger
 482 in cellular signal transduction. *Nature* **312**, 315-321.

483 **Bers, D. M.** (2002). Cardiac excitation-contraction coupling. *Nature* **415**, 198-205.

484 **Betzenhauser, M. J., Wagner, L. E., 2nd, Won, J. H. and Yule, D. I.** (2008). Studying
 485 isoform-specific inositol 1,4,5-trisphosphate receptor function and regulation. *Methods*
 486 **46**, 177-82.

487 **Bezprozvanny, I., Bezprozvannaya, S. and Ehrlich, B. E.** (1994). Caffeine-induced
 488 inhibition of inositol(1,4,5)-trisphosphate-gated calcium channels from cerebellum.
 489 *Mol. Biol. Cell* **5**, 97-103.

490 **Bezprozvanny, I. and Ehrlich, B. E.** (1994). Inositol (1,4,5)-trisphosphate (InsP₃)-gated Ca
 491 channels from cerebellum: conduction properties for divalent cations and regulation by
 492 intraluminal calcium. *J. Gen. Physiol.* **104**, 821-856.

493 **Bezprozvanny, I., Watras, J. and Ehrlich, B. E.** (1991). Bell-shaped calcium-response
 494 curves for Ins(1,4,5)P₃- and calcium-gated channels from endoplasmic reticulum of
 495 cerebellum. *Nature* **351**, 751-754.

496 **Bird, G. S. J. and Putney, J. W., Jr.** (1996). Effect of inositol 1,3,4,5-trisphosphate on
 497 inositol trisphosphate-activated Ca²⁺ signaling in mouse lacrimal cells. *J. Biol. Chem.*
 498 **271**, 6766-6770.

499 **Blondel, O., Takeda, J., Janssen, H., Seino, S. and Bell, G. I.** (1993). Sequence and
 500 functional characterization of a third inositol trisphosphate receptor subtype, IP₃R-3,
 501 expressed in pancreatic islets, kidney, gastrointestinal tract, and other tissues. *J. Biol.*
 502 *Chem.* **268**, 11356-11363.

503 **Bosanac, I., Alattia, J.-R., Mal, T. K., Chan, J., Talarico, S., Tong, F. K., Tong, K. I.,**
504 **Yoshikawa, F., Furuichi, T., Iwai, M. et al.** (2002). Structure of the inositol 1,4,5-
505 trisphosphate receptor binding core in complex with its ligand. *Nature* **420**, 696-700.

506 **Bosanac, I., Yamazaki, H., Matsu-ura, T., Michikawa, T., Mikoshiba, K. and Ikura, M.**
507 (2005). Crystal structure of the ligand binding suppressor domain of type 1 inositol
508 1,4,5-trisphosphate receptor. *Mol. Cell* **17**, 193-203.

509 **Burgess, G. M., Irvine, R. F., Berridge, M. J., McKinney, J. S. and Putney, J. W., Jr.**
510 (1984). Actions of inositol phosphates on calcium pools in guinea pig hepatocytes.
511 *Biochem. J.* **224**, 741-746.

512 **Burgess, G. M., McKinney, J. S., Fabiato, A., Leslie, B. A. and Putney, J. W., Jr.** (1983).
513 Calcium pools in saponin-permeabilized guinea pig hepatocytes. *J. Biol. Chem.* **258**,
514 15336-15345.

515 **Cao, Q., Yang, Y., Zhong, X. Z. and Dong, X. P.** (2017). The lysosomal Ca^{2+} release
516 channel TRPML1 regulates lysosome size by activating calmodulin. *J. Biol. Chem.*
517 **292**, 8424-8435.

518 **Champeil, P., Combettes, L., Berthon, B., Doucet, E., Orlowski, S. and Claret, M.**
519 (1989). Fast kinetics of calcium release induced by myo-inositol trisphosphate in
520 permeabilized rat hepatocytes. *J. Biol. Chem.* **264**, 17665-17673.

521 **Chandrasekhar, R., Alzayady, K. J., Wagner, L. E., 2nd and Yule, D. I.** (2016). Unique
522 regulatory properties of heterotetrameric inositol 1,4,5-trisphosphate receptors revealed
523 by studying concatenated receptor constructs. *J. Biol. Chem.* **291**, 4846-4860.

524 **Cheng, H. and Lederer, W. J.** (2008). Calcium sparks. *Physiol. Rev.* **88**, 1491-1545.

525 **Cheng, Y.-C. and Prusoff, W. H.** (1973). Relationship between the inhibition constant (K_I)
526 and the concentration of inhibitor causing 50 per cent inhibition (IC_{50}) of an enzymatic
527 reaction. *Biochem. Pharmacol.* **22**, 3099-3108.

528 **Cheung, K. H., Mei, L., Mak, D. O., Hayashi, I., Iwatsubo, T., Kang, D. E. and Foscett,**
529 **J. K.** (2010). Gain-of-function enhancement of IP_3 receptor modal gating by familial
530 Alzheimer's disease-linked presenilin mutants in human cells and mouse neurons. *Sci.*
531 *Signal.* **3**, ra22.

532 **Csordas, G., Weaver, D. and Hajnoczky, G.** (2018). Endoplasmic reticular-mitochondrial
533 contactology: structure and signaling functions. *Trends Cell Biol.* **28**, 523-540.

534 **de Azevedo, W. F., Jr. and Dias, R.** (2008). Experimental approaches to evaluate the
535 thermodynamics of protein-drug interactions. *Curr. Drug Targets* **9**, 1071-1076.

536 **Dehaye, J. P., Blackmore, P. F., Venter, J. C. and Exton, J. H.** (1980). Studies on the
 537 alpha-adrenergic activation of hepatic glucose output. alpha-adrenergic activation of
 538 phosphorylase by immobilized epinephrine. *J. Biol. Chem.* **255**, 3905-3910.

539 **Dellis, O., Dedos, S., Tovey, S. C., Rahman, T.-U., Dubel, S. J. and Taylor, C. W.**
 540 (2006). Ca^{2+} entry through plasma membrane IP_3 receptors. *Science* **313**, 229-233.

541 **Dellis, O., Rossi, A. M., Dedos, S. G. and Taylor, C. W.** (2008). Counting functional IP_3
 542 receptors into the plasma membrane. *J. Biol. Chem.* **283**, 751-755.

543 **des Georges, A., Clarke, O. B., Zalk, R., Yuan, Q., Condon, K. J., Grassucci, R. A.,**
 544 **Hendrickson, W. A., Marks, A. R. and Frank, J.** (2016). Structural basis for gating
 545 and activation of RyR1. *Cell* **167**, 145-157.

546 **Ding, Z., Rossi, A. M., Riley, A. M., Rahman, T., Potter, B. V. L. and Taylor, C. W.**
 547 (2010). Binding of inositol 1,4,5-trisphosphate (IP_3) and adenophostin A to the N-
 548 terminal region of the IP_3 receptor: thermodynamic analysis using fluorescence
 549 polarization with a novel IP_3 receptor ligand. *Mol. Pharmacol.* **77**, 995-1004.

550 **Dingwall, C. and Laskey, R.** (1992). The nuclear membrane. *Science* **258**, 942-947.

551 **Echevarria, W., Leite, M. F., Guerra, M. T., Zipfel, W. R. and Nathanson, M. H.** (2003).
 552 Regulation of calcium signals in the nucleus by a nucleoplasmic reticulum. *Nat. Cell*
 553 *Biol.* **5**, 440-446.

554 **Efremov, R. G., Leitner, A., Aebersold, R. and Raunser, S.** (2015). Architecture and
 555 conformational switch mechanism of the ryanodine receptor. *Nature* **517**, 39-43.

556 **Ehrlich, B. E. and Watras, J.** (1988). Inositol 1,4,5-trisphosphate activates a channel from
 557 smooth muscle sarcoplasmic reticulum. *Nature* **336**, 583-586.

558 **Endo, M., Tanaka, M. and Ogawa, Y.** (1970). Calcium induced release of calcium from the
 559 sarcoplasmic reticulum of skinned skeletal muscle fibres. *Nature* **228**, 34-36.

560 **Fabiato, A. and Fabiato, F.** (1979). Use of chlorotetracycline fluorescence to demonstrate
 561 Ca^{2+} -induced release of Ca^{2+} from sarcoplasmic reticulum of skinned cardiac cells.
 562 *Nature* **281**, 146-148.

563 **Fan, G., Baker, M. L., Wang, Z., Baker, M. R., Sinyagovskiy, P. A., Chiu, W., Ludtke,**
 564 **S. J. and Serysheva, I. I.** (2015). Gating machinery of InsP_3R channels revealed by
 565 electron cryomicroscopy. *Nature* **527**, 336-341.

566 **Ferris, C. D., Haganir, R. L., Supattapone, S. and Snyder, S. H.** (1989). Purified inositol
 567 1,4,5-trisphosphate receptor mediates calcium flux in reconstituted lipid vesicles.
 568 *Nature* **342**, 87-89.

569 **Feske, S., Gwack, Y., Prakriya, M., Srikanth, S., Puppel, S. H., Tanasa, B., Hogan, P.**
570 **G., Lewis, R. S., Daly, M. and Rao, A.** (2006). A mutation in Orai1 causes immune
571 deficiency by abrogating CRAC channel function. *Nature* **441**, 179-185.

572 **Fessenden, J. D., Chen, L., Wang, Y., Paolini, C., Franzini-Armstrong, C., Allen, P. D.**
573 **and Pessah, I. N.** (2001). Ryanodine receptor point mutant E4032A reveals an
574 allosteric interaction with ryanodine. *Proc. Natl. Acad. Sci. USA* **98**, 2865-2870.

575 **Foskett, J. K.** (2010). Inositol trisphosphate receptor Ca^{2+} release channels in neurological
576 diseases. *Pfluegers Arch./Eur. J. Physiol.* **460**, 481-494.

577 **Foskett, J. K., White, C., Cheung, K. H. and Mak, D. O.** (2007). Inositol trisphosphate
578 receptor Ca^{2+} release channels. *Physiol. Rev.* **87**, 593-658.

579 **Furuichi, T., Yoshikawa, S., Miyawaki, A., Wada, K., Maeda, M. and Mikoshiba, K.**
580 (1989). Primary structure and functional expression of the inositol 1,4,5-trisphosphate-
581 binding protein P_{400} . *Nature* **342**, 32-38.

582 **Furutama, D., Shimoda, K., Yoshikawa, S., Miyawaki, A., Furuichi, T. and Mikoshiba,**
583 **K.** (1996). Functional expression of the type 1 inositol 1,4,5-trisphosphate receptor
584 promoter-*lacZ* fusion genes in transgenic mice *J. Neurochem.* **66**, 1793-1801.

585 **Gin, E., Falcke, M., Wagner, L. E., 2nd, Yule, D. I. and Sneyd, J.** (2009). A kinetic model
586 of the inositol trisphosphate receptor based on single-channel data. *Biophys. J.* **96**,
587 4053-4062.

588 **Hagar, R. E., Burgstahler, A. D., Nathanson, M. H. and Ehrlich, B. E.** (1998). Type III
589 InsP_3 receptor channel stays open in the presence of increased calcium. *Nature* **296**, 81-
590 84.

591 **Hamada, K., Miyatake, H., Terauchi, A. and Mikoshiba, K.** (2017). IP_3 -mediated gating
592 mechanism of the IP_3 receptor revealed by mutagenesis and X-ray crystallography.
593 *Proc. Natl. Acad. Sci. USA* **114**, 4661-4666.

594 **Hou, X., Pedi, L., Diver, M. M. and Long, S. B.** (2012). Crystal structure of the calcium
595 release-activated calcium channel Orai. *Science* **338**, 1308-1313.

596 **Huang, P., Zou, Y., Zhong, X. Z., Cao, Q., Zhao, K., Zhu, M. X., Murell-Lagnado, R.**
597 **and Dong, X. P.** (2014). P_2X_4 forms functional ATP-activated cation channels on
598 lysosomal membranes regulated by luminal pH. *J. Biol. Chem.* **289**, 17658-17667.

599 **Iino, M.** (1987). Calcium dependent inositol trisphosphate-induced calcium release in the
600 guinea-pig taenia caeci. *Biochem. Biophys. Res. Commun.* **142**, 47-52.

- Iino, M.** (1990). Biphasic Ca^{2+} dependence of inositol 1,4,5-trisphosphate-induced Ca^{2+} release in smooth muscle cells of the guinea pig taenia caeci. *J. Gen. Physiol.* **95**, 1103-1122.
- Ionescu, L., White, C., Cheung, K. H., Shuai, J., Parker, I., Pearson, J. E., Foskett, J. K. and Mak, D. O.** (2007). Mode switching is the major mechanism of ligand regulation of InsP_3 receptor calcium release channels. *J. Gen. Physiol.* **130**, 631-635.
- Iwai, M., Michikawa, T., Bosanac, I., Ikura, M. and Mikoshiba, K.** (2007). Molecular basis of the isoform-specific ligand-binding affinity of inositol 1,4,5-trisphosphate receptors. *J. Biol. Chem.* **282**, 12755-12764.
- Jonas, E. A., Knox, R. J. and Kaczmarek, L.** (1997). Giga-ohm seals on intracellular membranes: a technique for studying intracellular ion channels in intact cells. *Neuron* **19**, 7-13.
- Knight, D. E.** (1981). Rendering cells permeable by exposure to electric fields. In *Techniques in Cellular Physiology*, pp. 1-20. Amsterdam: Elsevier/North Holland Scientific Publishers Ltd.
- Koulen, P., Cai, Y., Geng, L., Maeda, Y., Nishimura, S., Witzgall, R., Ehrlich, B.E. and Somlo, S.** (2002). Polycystin-2 is an intracellular calcium release channel. *Nat Cell Biol.* **4**, 191-197.
- Lai, F. A., Erickson, H. P., Rousseau, E., Liu, Q.-Y. and Meissner, G.** (1988). Purification and reconstitution of the calcium release channel from skeletal muscle. *Nature* **331**, 315-319.
- Lape, R., Colquhoun, D. and Sivilotti, L. G.** (2008). On the nature of partial agonism in the nicotinic receptor superfamily. *Nature* **454**, 722-727.
- Li, C., Enomoto, M., Rossi, A. M., Seo, M.-D., Rahman, T., Stathopoulos, P. B., Taylor, C. W., Ikura, M. and Ames, J. B.** (2013). CaBP1, a neuronal Ca^{2+} sensor protein, inhibits inositol trisphosphate receptors by clamping inter-subunit interactions. *Proc. Natl. Acad. Sci. USA* **110**, 8507-8512.
- Lin, C. C., Baek, K. and Lu, Z.** (2011). Apo and InsP_3 -bound crystal structures of the ligand-binding domain of an InsP_3 receptor. *Nat. Struct. Mol. Biol.* **18**, 1172-1174.
- Lock, J. T., Parker, I. and Smith, I. F.** (2015). A comparison of fluorescent Ca^{2+} indicators for imaging local Ca^{2+} signals in cultured cells. *Cell Calcium* **58**, 638-648.
- Loomis-Husselbee, J. W., Cullen, P. J., Dreikhausen, U. E., Irvine, R. F. and Dawson, A. P.** (1996). Synergistic effects of inositol 1,3,4,5-tetrakisphosphate on inositol 2,4,5-trisphosphate-stimulated Ca^{2+} release do not involve direct interaction of inositol

1,3,4,5-tetrakisphosphate with inositol trisphosphate-binding sites. *Biochem. J.* **314**, 811-816.

Ludtke, S. J., Serysheva, I. I., Hamilton, S. L. and Chiu, W. (2005). The pore structure of the closed RYR1 channel. *Structure* **13**, 1203-1211.

Ludtke, S. J., Tran, T. P., Ngo, Q. T., Moiseenkova-Bell, V. Y., Chiu, W. and Serysheva, I. I. (2011). Flexible architecture of IP₃R1 by cryo-EM. *Structure* **19**, 1192-1199.

Maeda, N., Kawasaki, T., Nakade, S., Yokota, N., Taguchi, T., Kasai, M. and Mikoshiba, K. (1991). Structural and functional characterization of inositol 1,4,5-trisphosphate receptor channel from mouse cerebellum. *J. Biol. Chem.* **266**, 1109-1116.

Maeda, N., Niinobe, M., Nakahira, K. and Mikoshiba, K. (1988). Purification and characterization of P₄₀₀ protein, a glycoprotein characteristic of purkinje cell from mouse cerebellum. *J. Neurochem.* **51**, 1724-1730.

Mak, D. O. and Foskett, J. K. (2014). Inositol 1,4,5-trisphosphate receptors in the endoplasmic reticulum: A single-channel point of view. *Cell Calcium* **58**, 67-78.

Mak, D. O., Pearson, J. E., Loong, K. P., Datta, S., Fernandez-Mongil, M. and Foskett, J. K. (2007). Rapid ligand-regulated gating kinetics of single inositol 1,4,5-trisphosphate receptor Ca²⁺ release channels. *EMBO Rep.* **8**, 1044-1051.

Mak, D. O., Vais, H., Cheung, K. H. and Foskett, J. K. (2013). Patch-clamp electrophysiology of intracellular Ca²⁺ channels. *Cold Spring Harbor Protocols* **2013**, 787-97.

Marchant, J., Callamaras, N. and Parker, I. (1999). Initiation of IP₃-mediated Ca²⁺ waves in *Xenopus* oocytes. *EMBO J.* **18**, 5285-5299.

Marchant, J. S. and Taylor, C. W. (1997). Cooperative activation of IP₃ receptors by sequential binding of IP₃ and Ca²⁺ safeguards against spontaneous activity. *Curr. Biol.* **7**, 510-518.

Marchenko, S. M., Yarotskyy, V. V., Kovalenko, T. N., Kostyuk, P. G. and Thomas, R. C. (2005). Spontaneously active and InsP₃-activated ion channels in cell nuclei from rat cerebellar Purkinje and granule neurones. *J. Physiol.* **565**, 897-910.

Mataragka, S. and Taylor, C. W. (2018). All three IP₃ receptor subtypes generate Ca²⁺ puffs, the universal building blocks of IP₃-evoked Ca²⁺ signals. *J. Cell Sci.* **In press**.

Meissner, G. (2017). The structural basis of ryanodine receptor ion channel function. *J. Gen. Physiol.* **149**, 1065-1089.

Meyer, T., Holowka, D. and Stryer, L. (1988). Highly cooperative opening of calcium channels by inositol 1,4,5-trisphosphate. *Science* **240**, 653-656.

669 **Michell, R. H.** (1975). Inositol phospholipids and cell surface receptor function. *Biochim.*
670 *Biophys. Acta* **415**, 81-147.

671 **Mignery, G. A. and Südhof, T. C.** (1990). The ligand binding site and transduction
672 mechanism in the inositol-1,4,5-trisphosphate receptor. *EMBO J.* **9**, 3893-3898.

673 **Mignery, G. A., Südhof, T. C., Takei, K. and De Camilli, P.** (1989). Putative receptor for
674 inositol 1,4,5-trisphosphate similar to ryanodine receptor. *Nature* **342**, 192-195.

675 **Miyakawa, T., Mizushima, A., Hirose, K., Yamazawa, T., Bezprozvanny, I., Kurosaki,**
676 **T. and Iino, M.** (2001). Ca^{2+} -sensor region of IP_3 receptor controls intracellular Ca^{2+}
677 signaling. *EMBO J.* **20**, 1674-1680.

678 **Monkawa, T., Miyawaki, A., Sugiyama, T., Yoneshima, H., Yamamoto-Hino, M.,**
679 **Furuichi, T., Saruta, T., Hasagawa, M. and Mikoshiba, K.** (1995). Heterotetrameric
680 complex formation of inositol 1,4,5-trisphosphate receptor subunits. *J. Biol. Chem.* **270**,
681 14700-14704.

682 **Morgan, A. J. and Galione, A.** (2013). Two-pore channels (TPCs): current controversies.
683 *Bioessays* **36**, 173-183.

684 **Nahorski, S. R. and Potter, B. V. L.** (1989). Molecular recognition of inositol
685 polyphosphates by intracellular receptors and metabolic enzymes. *Trends Pharmacol.*
686 *Sci.* **10**, 139-144.

687 **Neher, E.** (1992). Nobel lecture. Ion channels for communication between and within cells.
688 *EMBO J.* **11**, 1672-1679.

689 **Oxenoid, K., Dong, Y., Cao, C., Cui, T., Sancak, Y., Markhard, A. L., Grabarek, Z.,**
690 **Kong, L., Liu, Z., Ouyang, B. et al.** (2016). Architecture of the mitochondrial calcium
691 uniporter. *Nature* **533**, 269-273.

692 **Paknejad, N. and Hite, R. K.** (2018). Structural basis for the regulation of inositol
693 trisphosphate receptors by Ca^{2+} and IP_3 . *Nat. Struct. Mol. Biol.* **25**, 660-668.

694 **Parker, I. and Miledi, R.** (1989). Nonlinearity and facilitation in phosphoinositide signaling
695 studied by the use of caged inositol trisphosphate in *Xenopus* oocytes. *J. Neurosci.* **9**,
696 4068-4077.

697 **Patel, S., Harris, A., O'Beirne, G., Cook, N. D. and Taylor, C. W.** (1996). Kinetic analysis
698 of inositol trisphosphate binding to pure inositol trisphosphate receptors using
699 scintillation proximity assay. *Biochem. Biophys. Res. Commun.* **221**, 821-825.

700 **Patron, M., Raffaello, A., Granatiero, V., Tosatto, A., Merli, G., De Stefani, D., Wright,**
701 **L., Pallafacchina, G., Terrin, A., Mammucari, C. et al.** (2013). The mitochondrial

calcium uniporter (MCU): molecular identity and physiological roles. *J. Biol. Chem.* **288**, 10750-10758.

Peng, W., Shen, H., Wu, J., Guo, W., Pan, X., Wang, R., Chen, S. R. and Yan, N. (2016). Structural basis for the gating mechanism of the type 2 ryanodine receptor RyR2. *Science* **354**, aah5324.

Pinton, P., Pozzan, T. and Rizzuto, R. (1998). The Golgi apparatus is an inositol 1,4,5-trisphosphate-sensitive Ca^{2+} store, with functional properties distinct from those of the endoplasmic reticulum. *EMBO J.* **17**, 5298-5308.

Prakriya, M. and Lewis, R. S. (2015). Store-operated calcium channels. *Physiol. Rev.* **95**, 1383-1436.

Prole, D. L. and Taylor, C. W. (2016). Inositol 1,4,5-trisphosphate receptors and their protein partners as signalling hubs. *J. Physiol.* **594**, 2849-2866.

Putney, J. W., Jr. (1986). A model for receptor-regulated calcium entry. *Cell Calcium* **7**, 1-12.

Rahman, T., Skupin, A., Falcke, M. and Taylor, C. W. (2011). InsP₃R channel gating altered by clustering? Rahman *et al.* reply. *Nature* **478**, E2-E3.

Rahman, T. and Taylor, C. W. (2010). Nuclear patch-clamp recording from inositol 1,4,5-trisphosphate receptors. In *Calcium in Living Cells*, (ed. M. Whittaker), pp. 199-224. Amsterdam: Elsevier.

Rahman, T. U., Skupin, A., Falcke, M. and Taylor, C. W. (2009). Clustering of IP₃ receptors by IP₃ retunes their regulation by IP₃ and Ca^{2+} . *Nature* **458**, 655-659.

Ramos-Franco, J., Bare, D., Caenepeel, S., Nani, A., Fill, M. and Mignery, G. (2000). Single-channel function of recombinant type 2 inositol 1,4,5-trisphosphate receptor. *Biophys. J.* **79**, 1388-1399.

Ringer, S. (1883). A further contribution regarding the influence of the different constituents of the blood on the contraction of the heart. *J. Physiol.* **4**, 29-42.

Rios, E. (2018). Calcium-induced release of calcium in muscle: 50 years of work and the emerging consensus. *J. Gen. Physiol.* **150**, 521-537.

Rizzuto, R., De Stefani, D., Raffaello, A. and Mammucari, C. (2012). Mitochondria as sensors and regulators of calcium signalling. *Nat. Rev. Mol. Cell Biol.* **13**, 566-578.

Rodriguez, E. A., Campbell, R. E., Lin, J. Y., Lin, M. Z., Miyawaki, A., Palmer, A. E., Shu, X., Zhang, J. and Tsien, R. Y. (2017). The growing and glowing toolbox of fluorescent and photoactive proteins. *Trends Biochem. Sci.* **42**, 111-129.

Rossi, A. M., Riley, A. M., Potter, B. V. L. and Taylor, C. W. (2010). Adenophostins: high-affinity agonists of IP₃ receptors. *Curr. Top. Membr.* **66**, 209-233.

Rossi, A. M., Riley, A. M., Tovey, S. C., Rahman, T., Dellis, O., Taylor, E. J. A., Veresov, V. G., Potter, B. V. L. and Taylor, C. W. (2009). Synthetic partial agonists reveal key steps in IP₃ receptor activation. *Nat. Chem. Biol.* **5**, 631-639.

Rossi, A. M. and Taylor, C. W. (2013). High-throughput fluorescence polarization assay of ligand binding to IP₃ receptors. *Cold Spring Harbor Protocols* **2013**, 938-946.

Rossi, A. M., Tovey, S. C., Rahman, T., Prole, D. L. and Taylor, C. W. (2012). Analysis of IP₃ receptors in and out of cells. *Biochim. Biophys. Acta* **1820**, 1214-1227.

Saleem, H., Tovey, S. C., Molinski, T. F. and Taylor, C. W. (2014). Interactions of antagonists with subtypes of inositol 1,4,5-trisphosphate (IP₃) receptor. *Br. J. Pharmacol.* **171**, 3298-3312.

Saleem, H., Tovey, S. C., Rahman, T., Riley, A. M., Potter, B. V. L. and Taylor, C. W. (2012). Stimulation of inositol 1,4,5-trisphosphate (IP₃) receptor subtypes by analogues of IP₃. *PLoS ONE* **8**, e54877.

Schug, Z. T. and Joseph, S. K. (2006). The role of the S4-S5 linker and C-terminal tail in inositol 1,4,5-trisphosphate receptor function. *J. Biol. Chem.* **281**, 24431-24440.

Schulz, I. (1990). Permeabilizing cells: some methods and application for the study of intracellular processes. *Methods Enzymol.* **192**, 280-300.

Seo, M.-D., Velamakanni, S., Ishiyama, N., Stathopoulos, P. B., Rossi, A. M., Khan, S. A., Dale, P., Li, C., Ames, J. B., Ikura, M. et al. (2012). Structural and functional conservation of key domains in InsP₃ and ryanodine receptors. *Nature* **483**, 108-112.

Smith, I. F. and Parker, I. (2009). Imaging the quantal substructure of single IP₃R channel activity during Ca²⁺ puffs in intact mammalian cells. *Proc. Natl. Acad. Sci. USA* **106**, 6404-6409.

Smith, I. F., Wiltgen, S. M., Shuai, J. and Parker, I. (2009). Ca²⁺ puffs originate from preestablished stable clusters of inositol trisphosphate receptors. *Sci. Signal.* **2**, ra77.

Spät, A., Bradford, P. G., McKinney, J. S., Rubin, R. P. and Putney, J. W., Jr. (1986). A saturable receptor for ³²P-inositol-1,4,5-trisphosphate in hepatocytes and neutrophils. *Nature* **319**, 514-516.

Stehno-Bittel, L., Lückhoff, A. and Clapham, D. E. (1995). Calcium release from the nucleus by InsP₃ receptor channels. *Neuron* **14**, 163-167.

767 **Streb, H., Irvine, R. F., Berridge, M. J. and Schulz, I.** (1983). Release of Ca^{2+} from a
768 nonmitochondrial intracellular store in pancreatic acinar cells by inositol-1,4,5-
769 trisphosphate. *Nature* **306**, 67-69.

770 **Südhof, T. C., Newton, C. L., Archer, B. T., Ushkaryov, Y. A. and Mignery, G. A.**
771 (1991). Structure of a novel InsP_3 receptor. *EMBO J.* **10**, 3199-3206.

772 **Supattapone, S., Worley, P. F., Baraban, J. M. and Snyder, S. H.** (1988). Solubilization,
773 purification, and characterization of an inositol trisphosphate receptor. *J. Biol. Chem.*
774 **263**, 1530-1534.

775 **Sureshan, K. M., Riley, A. M., Thomas, M. P., Tovey, S. C., Taylor, C. W. and Potter, B.**
776 **V.** (2012). Contribution of phosphates and adenine to the potency of adenophostins at
777 the IP_3 receptor: synthesis of all possible bisphosphates of adenophostin A. *J. Med.*
778 *Chem.* **55**, 1706-1720.

779 **Takahashi, M., Tanzawa, K. and Takahashi, S.** (1994). Adenophostins, newly discovered
780 metabolites of *Penicillium brevicompactum*, act as potent agonists of the inositol 1,4,5-
781 trisphosphate receptor. *J. Biol. Chem.* **269**, 369-372.

782 **Taylor, C. W., Prole, D. L. and Rahman, T.** (2009). Ca^{2+} channels on the move.
783 *Biochemistry* **48**, 12062-12080.

784 **Taylor, C. W., Tovey, S. C., Rossi, A. M., Lopez Sanjurjo, C. I., Prole, D. L. and**
785 **Rahman, T.** (2014). Structural organization of signalling to and from IP_3 receptors.
786 *Biochem. Soc. Trans.* **42**, 63-70.

787 **Terry, L. E., Alzayady, K. J., Furati, E. and Yule, D. I.** (2018). Inositol 1,4,5-
788 trisphosphate receptor mutations associated with human disease. *Messenger* **6**, 29-44.

789 **Thillaiappan, N. B., Chavda, A. P., Tovey, S. C., Prole, D. L. and Taylor, C. W.** (2017).
790 Ca^{2+} signals initiate at immobile IP_3 receptors adjacent to ER-plasma membrane
791 junctions. *Nat. Commun.* **8**, 1505.

792 **Thorn, K.** (2016). A quick guide to light microscopy in cell biology. *Mol. Biol. Cell* **27**, 219-
793 222.

794 **Thurley, K., Tovey, S. C., Moenke, G., Prince, V. L., Meena, A., Thomas, A. P., Skupin,**
795 **A., Taylor, C. W. and Falcke, M.** (2014). Reliable encoding of stimulus intensities
796 within random sequences of intracellular Ca^{2+} spikes. *Sci. Signal.* **7**, ra59.

797 **Uchida, K., Miyauchi, H., Furuichi, T., Michikawa, T. and Mikoshiba, K.** (2003).
798 Critical regions for activation gating of the inositol 1,4,5-trisphosphate receptor. *J. Biol.*
799 *Chem.* **278**, 16551-16560.

800 **Vais, H., Foskett, J. K. and Mak, D. O.** (2011). InsP₃R channel gating altered by
801 clustering? *Nature* **478**, E1-E2.

802 **Van Petegem, F.** (2014). Ryanodine receptors: allosteric ion channel giants. *J. Mol. Biol.*
803 **427**, 31-53.

804 **Wassler, M., Jonasson, I., Persson, R. and Fries, E.** (1987). Differential permeabilization
805 of membranes by saponin treatment of isolated rat hepatocytes. Release of secretory
806 vesicles. *Biochem. J.* **247**, 407-415.

807 **Watras, J., Bezprozvanny, I. and Ehrlich, B. E.** (1991). Inositol 1,4,5-trisphosphate-gated
808 channels in cerebellum: presence of multiple conductance states. *J. Neurosci.* **11**, 3239-
809 3245.

810 **Worley, P. F., Baraban, J. M., Supattapone, S., Wilson, V. S. and Snyder, S. H.** (1987).
811 Characterization of inositol trisphosphate receptor binding in brain. Regulation by pH
812 and calcium. *J. Biol. Chem.* **262**, 12132-12136.

813 **Xie, X., Xu, A. M., Leal-Ortiz, S., Cao, Y., Garner, C. C. and Melosh, N. A.** (2013).
814 Nanostraw-electroporation system for highly efficient intracellular delivery and
815 transfection. *ACS Nano* **7**, 4351-4358.

816 **Yamazaki, H., Chan, J., Ikura, M., Michikawa, T. and Mikoshiba, K.** (2010). Tyr-
817 167/Trp-168 in type1/3 inositol 1,4,5-trisphosphate receptor mediates functional
818 coupling between ligand binding and channel opening. *J. Biol. Chem.* **285**, 36081-
819 36091.

820 **Yan, Z., Bai, X. C., Yan, C., Wu, J., Li, Z., Xie, T., Peng, W., Yin, C. C., Li, X., Scheres,**
821 **S. H. et al.** (2015). Structure of the rabbit ryanodine receptor RyR1 at near-atomic
822 resolution. *Nature* **517**, 50-55.

823 **Yen, M. and Lewis, R. S.** (2018). Physiological CRAC channel activation and pore
824 properties require STIM1 binding to all six Orai1 subunits. *J. Gen. Physiol.* **In press**.

825 **Yoshikawa, F., Morita, M., Monkawa, T., Michikawa, T., Furuichi, T. and Mikoshiba,**
826 **K.** (1996). Mutational analysis of the ligand binding site of the inositol 1,4,5-
827 trisphosphate receptor. *J. Biol. Chem.* **271**, 18277-18284.

828 **Zalk, R., Clarke, O. B., Georges, A. D., Grassucci, R. A., Reiken, S., Mancina, F.,**
829 **Hendrickson, W. A., Frank, J. and Marks, A. R.** (2015). Structure of a mammalian
830 ryanodine receptor. *Nature* **517**, 44-49.

831 **Zsolnay, V., Fill, M. and Gillespie, D.** (2018). Sarcoplasmic reticulum Ca²⁺ release uses a
832 cascading network of intra-SR and channel countercurrents. *Biophys. J.* **114**, 462-473.

Fig. 1: Ca^{2+} release by IP_3 and ryanodine receptors. (A) Many receptors in the plasma membrane (PM), including G-protein-coupled receptors (GPCRs) and receptor tyrosine kinases (RTKs), stimulate phospholipases C (PLC), causing hydrolysis of the PM lipid, phosphatidylinositol 4,5-bisphosphate, into diacylglycerol and IP_3 . IP_3 binds to each of the four IP_3 -binding sites of the tetrameric IP_3R to initiate conformational changes that lead to channel opening and release of Ca^{2+} from the ER. IP_3 is deactivated by phosphorylation to IP_4 or dephosphorylation to IP_2 . RyRs are close relatives of IP_3Rs , but they are predominantly expressed in the sarcoplasmic reticulum of skeletal (RyR1) and cardiac (RyR2) muscle. Each RyR is activated when depolarization of the PM activates voltage-gated Ca^{2+} channels (Ca_v1). RyR1 are directly activated by conformational coupling to $\text{Ca}_v1.1$, whereas Ca^{2+} entering cardiac myocytes through $\text{Ca}_v1.2$ activates RyR2 through Ca^{2+} -induced Ca^{2+} release (CICR). Structures from Electron Microscopy Data Bank (IP_3R , EMD-5278 (Ludtke et al., 2011); RyR1, EMD-1275 (Ludtke et al., 2005)). (B) IP_3 binding is not alone sufficient to activate IP_3Rs . IP_3 binding primes IP_3Rs to bind Ca^{2+} and that leads to channel opening. All four IP_3 -binding sites must be occupied for the pore to open, but it is not yet known how many Ca^{2+} -binding sites must be occupied (we show four for simplicity). (C) Dual regulation of IP_3Rs by IP_3 and Ca^{2+} allows them to propagate regenerative Ca^{2+} signals by CICR. Local CICR activity within a small cluster of IP_3Rs generates a Ca^{2+} puff. (D) The vicinal 4,5-bisphosphate moiety of IP_3 is essential for activity, whereas the 1-phosphate enhances affinity. (E) IP_3 is recognised by the IP_3 -binding core (IBC) of IP_3R . The essential 4- and 5-phosphates of IP_3 interact with opposing sides of the clam-like IBC to cause clam closure. The loop of the suppressor domain (SD) interacts with IBC- β of a neighbouring subunit (Seo et al., 2012). A-C modified from Taylor et al. (2014), and D reproduced from Seo et al. (2012).

Fig. 2: Measuring IP₃ binding to IP₃Rs. (A) Binding assays allow determination of the equilibrium dissociation constant (K_D) (**Box 2**). Non-equilibrium measurements allow rate constants (k_{+1} and k_{-1}) to be determined. (B) Commonly, radioactive IP₃ (typically ³H-IP₃) is equilibrated with IP₃R before rapidly separating (usually by centrifugation) bound and free ligands to determine the amount of ³H-IP₃ bound to its receptor. (C) By immobilizing IP₃R on the surface of a bead that detects only immediately adjacent (i.e. bound) ³H-IP₃, scintillation proximity assays (SPA) report bound ³H-IP₃ without separating bound from free ligand (Patel et al., 1996). (D) A variety of methods, including surface-plasmon resonance (SPR), fluorescence correlation spectroscopy (FCS) and fluorescence polarization (FP) rely on detecting the large increase in apparent size of IP₃ as it binds to the IP₃R (or a fragment of it). With FP, for example (illustrated), a fluorescent analogue of IP₃ rotates rapidly when free, but less so when it has bound to a soluble IP₃R fragment. The difference can be measured, without separating bound and free ligands, by recording the extent to which plane-polarized light remains polarized (Ding et al., 2010). (E) Isothermal titration calorimetry (ITC) measures the very small amounts of heat released or absorbed (ΔH) as IP₃ binds to purified IP₃R by comparison with a reference cell (de Azevedo and Dias, 2008).

Fig. 3: Towards understanding how IP₃ and Ca²⁺ open IP₃Rs. (A) Single IP₃R1 subunit showing key domains: the N-terminal suppressor domain (SD); the β and α domains of the IP₃-binding core (IBC); the intervening lateral domain (ILD), which lies between ARM3 and the first trans-membrane domain (TMD1); TMD6, which lines the pore and is occluded by hydrophobic residues towards its cytosolic end in the closed state; the helical linker domain (LNK); and the C-terminal α -helical domain (CTD), which is unique to IP₃Rs. The structure was published in Fan et al. (2015) (Protein Data Base, PDB 3JAV). (B) Simplified scheme, derived from structures of IP₃R1 (Fan et al., 2015) and IP₃R3 (Paknejad and Hite, 2018) shows that the only contact between the cytosolic and pore region occurs at the nexus between ARM3 with its C-terminal ILD domain and the C-terminal extension of TMD6 (LNK). These contacts form an interleaved structure, with residues from LNK and the base of ARM3 cooperating to form a Ca²⁺-binding site. Binding sites for IP₃ (IBC- α and IBC- β) and Ca²⁺ are formed by residues contributed from different domains, allowing rigid-body movements of domains to reconfigure the sites. The first Ca²⁺-binding site assembles from residues provided by ARM1 and the α -helical linker between ARM1 and ARM2. The second Ca²⁺-binding site is structurally conserved in RyR, and assembled by residues from ARM3 and LNK domains. This second site may mediate the IP₃-regulated binding of Ca²⁺ that precedes channel opening (see text for details) (Paknejad and Hite, 2018). Opening of the pore requires movement of occluding hydrophobic residues that lie close to the cytosolic end of TMD6; Ca²⁺ can then pass rapidly from the ER lumen to the cytosol.

Box 1: IP₃Rs and RyRs are not the only intracellular Ca²⁺ channels

IP₃Rs and RyRs are the major intracellular Ca²⁺-release channels in most cells and the major links between extracellular stimuli and Ca²⁺ release from the ER or sarcoplasmic reticulum (SR) (**Fig. 1A**), but they are not the only intracellular Ca²⁺ channels (Taylor et al., 2009). Polycystin-2 (also known as TRPP2), a member of the transient receptor potential (TRP) superfamily, is also expressed in the ER and is activated by Ca²⁺ (Koulen et al., 2002). A variety of Ca²⁺-permeable channels are expressed in lysosomes, including those regulated by luminal pH and ATP (P2X purinoceptor 4, P2X4) (Huang et al., 2014), cytosolic nicotinic acid adenine dinucleotide phosphate (NAADP; two pore channel 2, TPC2) (Morgan and Galione, 2013), and the lysosomal membrane lipid, phosphatidylinositol 3,5-bisphosphate (transient receptor potential mucolipin 1 channel, TRPML1) (Cao et al., 2017). The mitochondrial uniporters (MCU) comprise another important family of intracellular Ca²⁺ channels (Oxenoid et al., 2016; Patron et al., 2013). Opening of MCU is triggered by large local increases in [Ca²⁺]_c, causing Ca²⁺ to flow rapidly from the cytosol across the inner mitochondrial membrane and into the mitochondrial matrix, where Ca²⁺ regulates many activities (Rizzuto et al., 2012). A recurrent theme in Ca²⁺ signalling is the importance of interactions between Ca²⁺ channels in different membranes: store-operated Ca²⁺ entry is activated after loss of Ca²⁺ from the ER through IP₃Rs; mitochondrial Ca²⁺ uptake is driven by local Ca²⁺ release through IP₃Rs and RyRs (Csordas et al., 2018); NAADP-evoked Ca²⁺ release from lysosomes is amplified by CICR through closely apposed IP₃Rs or RyRs (Morgan and Galione, 2013); and Ca²⁺ puffs and sparks are ignited by CICR triggering Ca²⁺ release within clusters of IP₃Rs or RyRs (**Fig. 1C**) (Cheng and Lederer, 2008; Rios, 2018; Thillaiappan et al., 2017).

Box 2: Analysis of IP₃ binding

Analyses of IP₃ binding allow affinities of IP₃ or competing ligands to be determined (as equilibrium dissociation constants, K_D , the concentration of IP₃ at which 50% of binding sites are occupied) (**Fig. 2**). These analyses determine the relationship between the concentration of a ligand and the amount bound to IP₃Rs. Radioligand binding, using ³H-IP₃, is the most commonly used approach. Most methods used to determine specific binding of ³H-IP₃ to IP₃Rs require rapid separation of bound and free ³H-IP₃, such that the equilibrium between free ³H-IP₃, competing ligands and the IP₃R is not perturbed by the separation procedure (filtration or centrifugation) (**Fig. 2A,B**). Measuring specific binding with different concentrations of ³H-IP₃ allows the K_D for ³H-IP₃ to be determined, whereas measuring specific binding of ³H-IP₃ in the presence of different concentrations of a competing ligand allow the K_D of that ligand to be determined (Cheng and Prusoff, 1973). Advantages of these ³H-IP₃ binding assays are their simplicity and applicability to IP₃Rs within membranes, after detergent-solubilization or as IP₃-binding fragments (Rossi et al., 2009). Scintillation proximity assays (SPA) avoid the need for separation steps because the SPA beads are impregnated with a scintillant, such that when IP₃Rs are immobilized on the surface of the bead, only ³H-IP₃ bound to an IP₃R is detected (**Fig. 2C**) (Patel et al., 1996). More specialized methods allow analysis of ligand binding to IP₃Rs without using radioligands. These methods include fluorescence polarization (FP), which uses a fluorescent analogue of IP₃ to report the size of the molecule to which the fluorophore is attached. When free, the fluorescent IP₃ is small and tumbles rapidly in solution, but when bound to a large IP₃R fragment it tumbles more slowly. These changes can be detected using plane-polarized light (**Fig. 2D**) (Ding et al., 2010; Rossi and Taylor, 2013). Isothermal titration calorimetry (ITC), which measures heat exchange during IP₃ binding, is another means of measuring ligand binding to IP₃Rs without using ³H-IP₃ (**Fig. 2E**) (de Azevedo and Dias, 2008). Limitations of both FP and ITC include the need for both specialised equipment and large amounts of purified protein.

Box 3: Nuclear patch-clamp recordings can be applied to IP₃Rs

Patch-clamp recording allows the opening and closing of single ion channels to be recorded with exquisite sensitivity (Neher, 1992). Usually these recordings are made at the plasma membrane (PM), but that is not applicable to single-channel recordings from IP₃Rs, most of which are expressed in ER. However, the outer nuclear membrane (ONM) is continuous with the ER membrane, and IP₃Rs are expressed in the ONM. A glass microelectrode applied to the ONM of an isolated nucleus allows single-channel recording from IP₃Rs trapped within. By excising the patch from the intact nucleus to provide an excised patch, it is possible to make recordings with the IP₃-binding site of the IP₃R exposed to either the interior of the patch-pipette patch or (with greater difficulty) to the bath solution (Mak et al., 2007). The latter allows rapid application of IP₃ or Ca²⁺ to the cytosolic surface. K⁺ or Cs⁺ are commonly used as charge-carriers for patch-clamp recording because they provide large currents and they, unlike Ca²⁺, do not regulate IP₃R gating. These patch-clamp methods allow the ion selectivity and conductance of IP₃Rs to be determined. By examining the sequence of channel openings and closing, gating schemes can be developed that seek to explain how regulators of IP₃Rs (like IP₃ and Ca²⁺) move the channel through different closed states to its open state (Mak and Foskett, 2014; Rahman et al., 2009). Image reproduced, with permission, from Rossi et al. (2012).

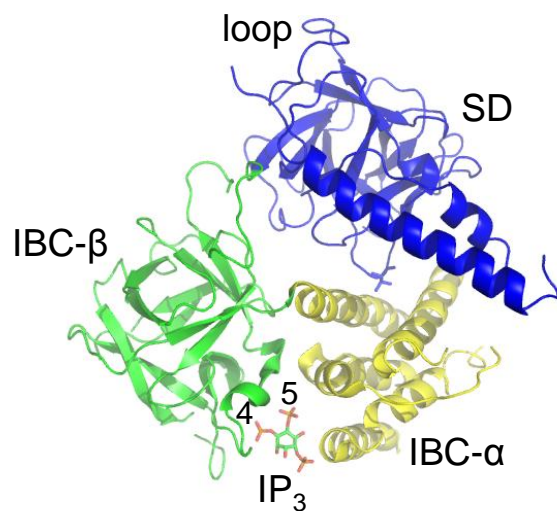
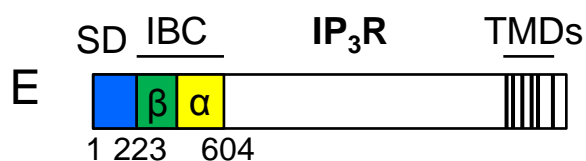
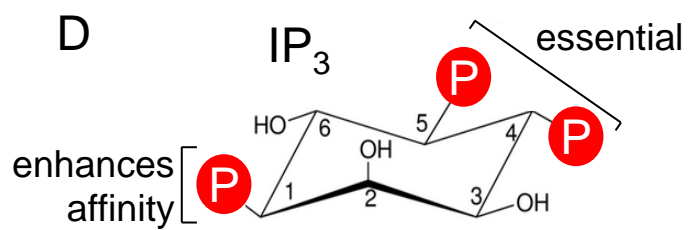
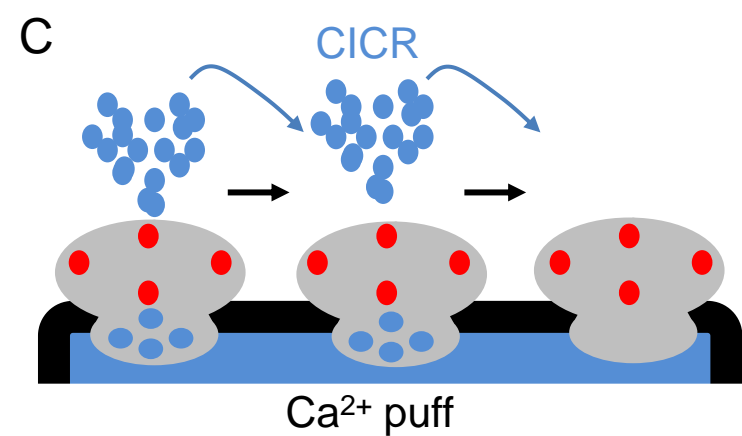
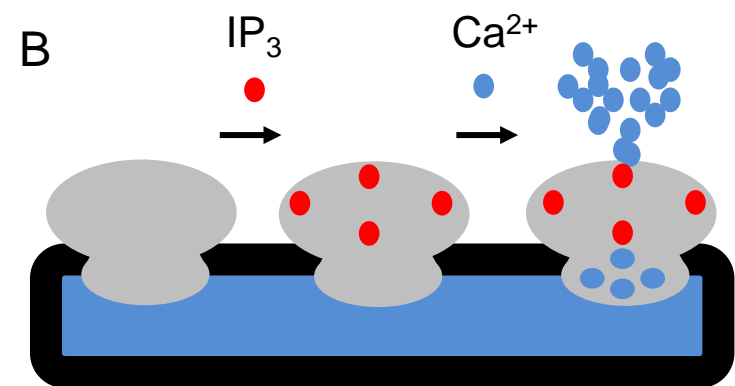
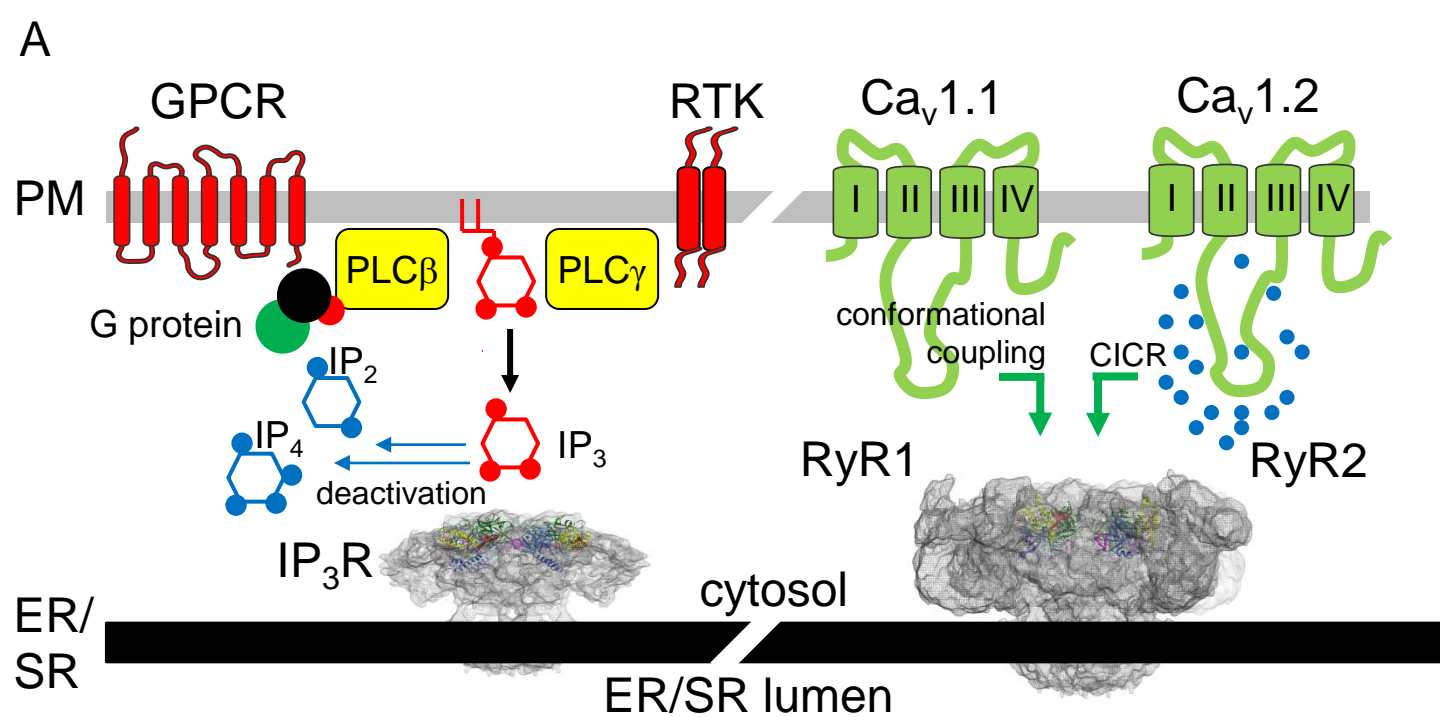


Figure 1

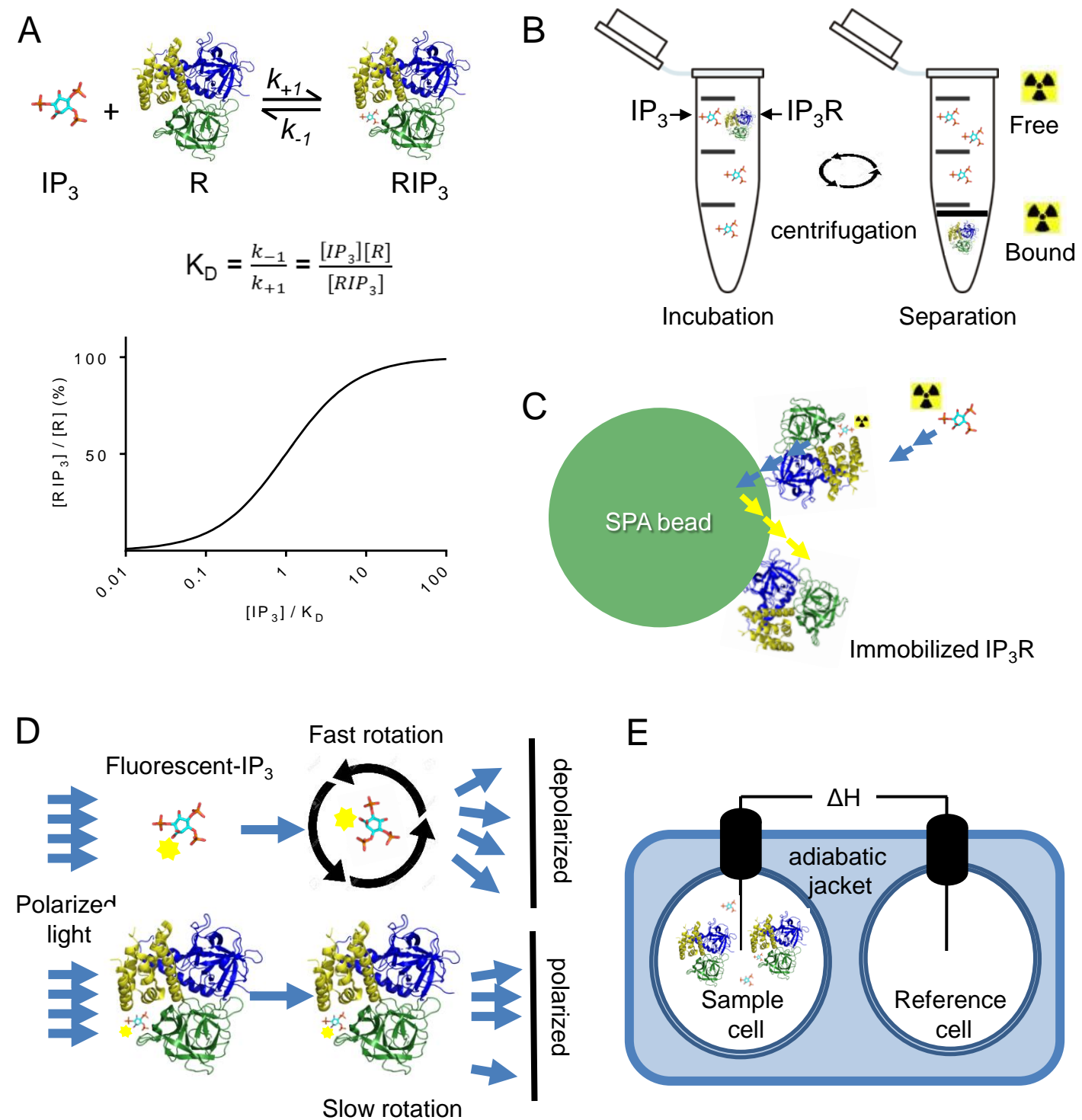


Figure 2

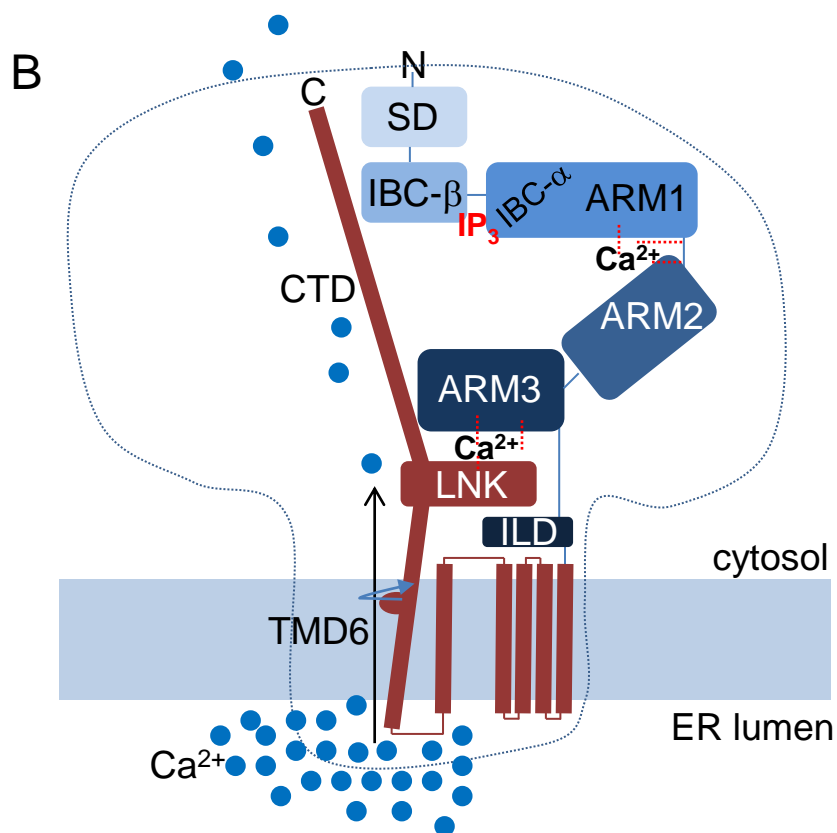
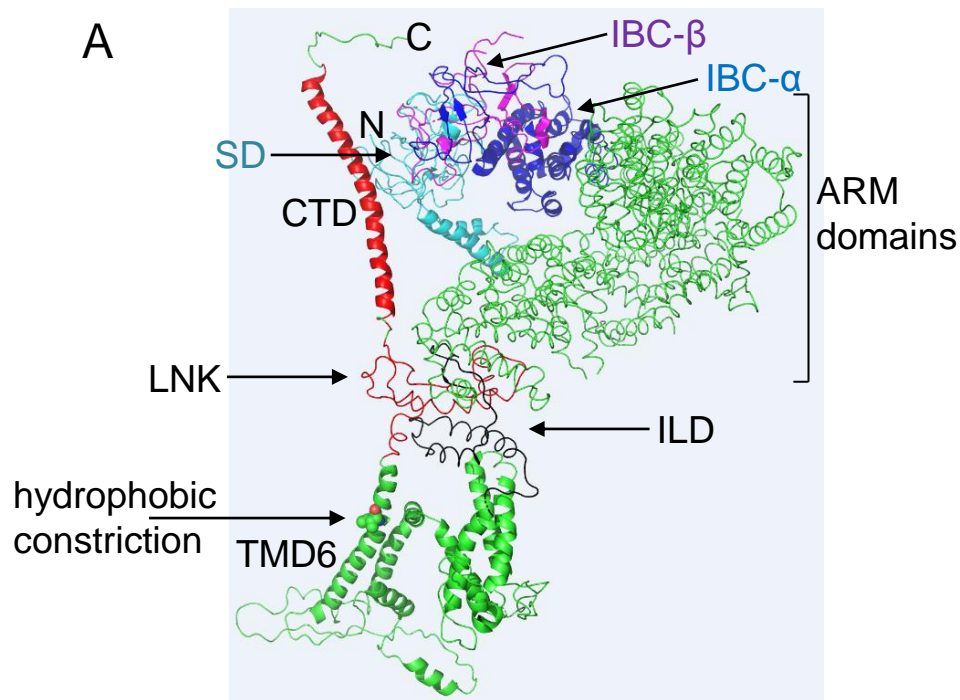


Figure 3

